Supplementary Information for Optimizing Adsorption Refrigeration with MOF-Propane Integration: A Sustainable Approach

S Muthu Krishnan,[†] Riya Sharma,[†] and Jayant K. Singh[*,†,‡]

[†]*Department of Chemical Engineering, Indian Institute of Technology Kanpur, Uttar Pradesh, 208016, India*

[‡]*Prescience Insilico Private Limited, 5th Floor, Novel MSR Building, Marathalli, Bengaluru, Karnataka, 560037, India.*

E-mail: jayantks@iitk.ac.in

Phone: +91 (0)512 2596141. Fax: +91-512-2590104

Contents

S1 Theory

S1.1 Adsorption Refrigeration Cycle

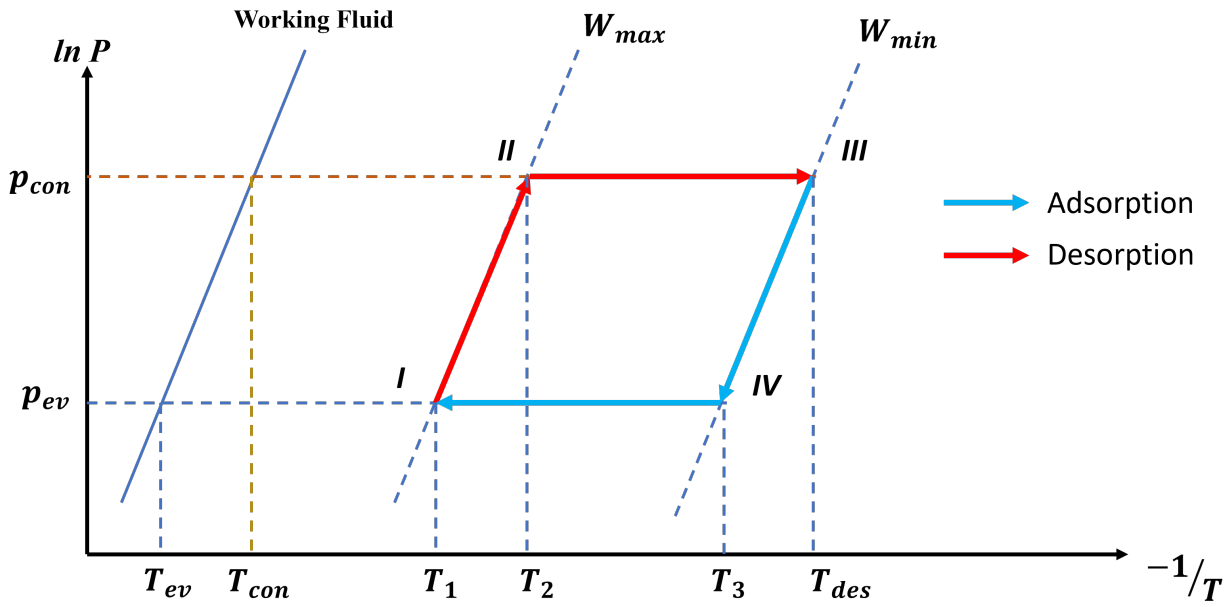

Fig. S1: Representation of an adsorption refrigeration cycle, following Clausius Clapeyron equation. T_{ev} and T_{con} are the operating temperatures of the evaporator and the condenser respectively, T_1 is the operating temperature of the adsorbent bed, T_{des} is the desorption temperature. T_2 is the minimal desorption or maximal pre-heating temperature calculated by the Trouton's rule.

An adsorption refrigeration cycle goes through 4 stages (i) I - II Isosteric Heating (ii) II - III Isobaric Desorption (iii) III - IV Isosteric Cooling (iv) IV - I Isobaric Adsorption.

S1.1.1 Isosteric Heating (I - II)

At point, I, the adsorbent bed achieves full adsorption at a temperature of $T_1 = T_{ads}$, corresponding to the ambient temperature at which the adsorbent bed is maintained. In practical conditions, $T_{con} = T_1 = T_{ads}$, and the uptake at this condition is denoted by W_{max}. Subsequently, the adsorbent bed is disengaged from the evaporator and condenser, undergoing constant heating until the pressure within the bed reaches p_{con}, which is depicted

as point II. At this juncture, the adsorbent bed attains a temperature of T_2 and a pressure of p_{con}. The energy required for heating is represented as Q_1. The determination of T_2 involves the application of Trouton's rule.[2]

$$T_{con}^2 = (T_2 * T_{ev}) \tag{1}$$

S1.1.2 Isobaric Desorption (II - III)

The adsorbent bed, under continuous heating, is coupled with the condenser. Heating is continued until the temperature within the adsorbent bed reaches T_{des}. The energy input for this heating process is quantified by Q_2. Concurrently, the desorbed refrigerant gas is directed to the condenser, leading to a reduction in uptake from W_{max} to W_{min}. When the system reaches point III the adsorbent bed is at a temperature T_{des} and pressure p_{con} exhibiting an uptake of W_{min}. At III, the adsorbent bed is completely desorbed. The refrigerant goes into the condenser, where it condenses, and is stored in the refrigerant tank.

S1.1.3 Isosteric Cooling (III - IV)

Once the adsorbent bed has been cooled down, it becomes ready for adsorption when the internal pressure reaches p_{ev}, the operational pressure of the evaporator; the accompanying energy release in this stage is denoted as Q_3. The adsorbent bed is then kept isolated by disconnecting it from the condenser and the evaporator and allowed to cool down until it reaches point IV. This cooling process occurs at a constant uptake of W_{min}.

S1.1.4 Isobaric Adsorption (IV - I)

During this phase, the refrigerant gas undergoes the adsorption process within the connected adsorbent bed linked to the evaporator. The adsorbent bed gradually captures the refrigerant gas, releasing heat and consequently cooling the adsorbent bed. The energy liberated in this stage is given by Q_4. When the system reaches point I, the adsorbent bed is at a temperature

of T_{ads} and a pressure of p_{ev} with an uptake of W_{max}.

S1.2 Thermodynamic Modelling

The efficiency of this cycle is determined by calculating the coefficient of performance (COP). The same cycle can be used to describe the adsorption heat pump and adsorption refrigeration cycles. The only difference is the direction of heat transfer. The COP of the two cycles can be given by.[2–4]

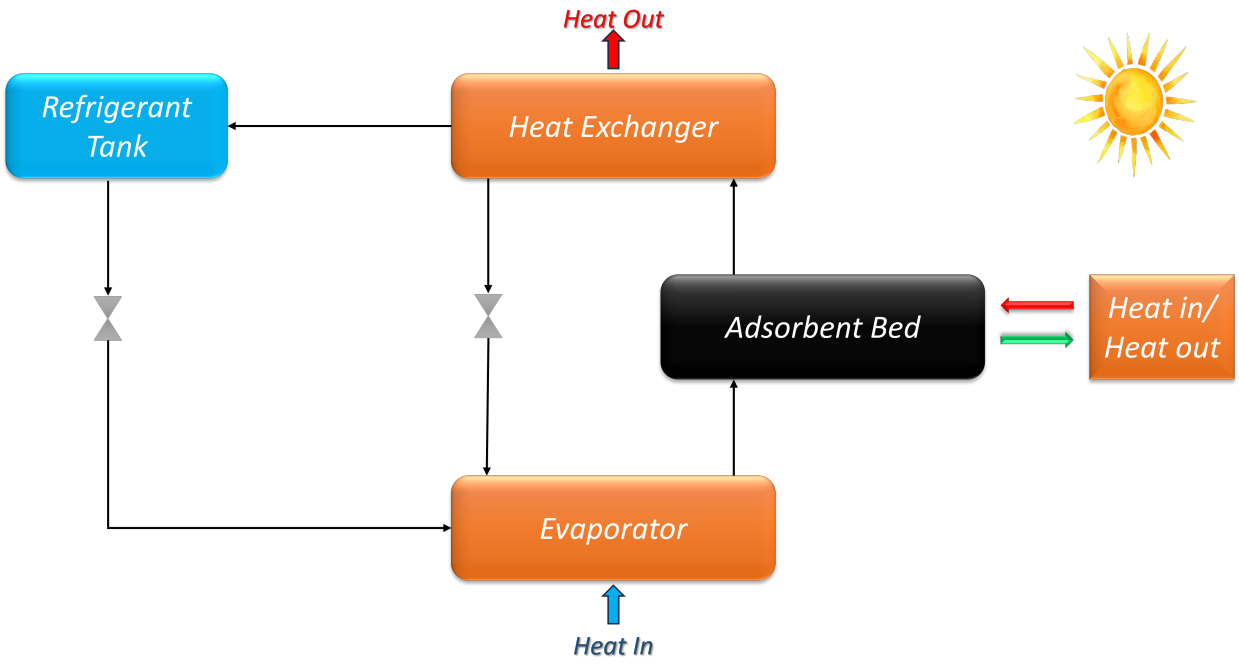

Fig. S2: A schematic representation of the adsorption refrigeration (AR) cycle

$$COP_H = \frac{-(Q_{con} + Q_{ads})}{Q_{reg}} \tag{2}$$

$$COP_R = \frac{Q_{ev}}{Q_{reg}} \tag{3}$$

Where Q_{con} is the energy released during condensation, Q_{ads} is the energy released during the adsorption stage, both are negative as energy is released. Q_{reg} is the energy required to

regenerate the fully adsorbed adsorbent bed. This is given by,[3]

$$Q_{reg} = Q_1 + Q_2 - Q_{sorption} \tag{4}$$

where Q_1 is energy required for heating from I-II, Q_2 is the energy required for heating from II-III and $Q_{sorption}$ is the energy released during the adsorption of the working fluid.

The energies represented in terms of measurable quantities like uptake W, heat of adsorption ΔH_{ads}, heat capacity C_p, and the density of the working fluid ρ_{liq}^{wf} are given by,[2,5]

$$Q_1 = m_{sorbent} C_p^{sorbent} (T_2 - T_1) + m_{sorbent} q_{max} C_p^{wf} (T_2 - T_1) \tag{5}$$

$$Q_2 = m_{sorbent} C_p^{sorbent} (T_{des} - T_2) + m_{sorbent} \frac{q_{max} + q_{min}}{2} C_p^{wf} (T_{des} - T_2) \tag{6}$$

$$Q_{sorption} = \frac{m_{sorbent} \Delta q < \Delta H_{ads} >}{M_w} \tag{7}$$

where q the uptake is given by Gurvich rule[5] as,

$$q = W \rho_{liq}^{wf} \tag{8}$$

Q_{ev} the energy taken from the evaporator is given by,[3]

$$Q_{ev} = -\frac{m_{sorbent} \Delta H_{vap}(T_{ev}) \Delta q}{M_w} \tag{9}$$

Q_{con} the energy released to the condenser is given by,[3]

$$Q_{con} = \frac{m_{sorbent} \Delta H_{vap}(T_{con}) \Delta q}{M_w} \tag{10}$$

Now the final equation for the COP_R for the adsorption refrigeration cycle will be,

$$COP_R = \frac{\frac{m_{sorbent}\Delta H_{vap}(T_{ev})\Delta q}{M_w}}{\begin{aligned} &m_{sorbent}C_p^{sorbent}(T_{des}-T_1) + m_{sorbent}q_{max}C_p^{wf}(T_2-T_1)+ \\ &m_{sorbent}\frac{q_{max}+q_{min}}{2}C_p^{wf}(T_{des}-T_2) - \frac{m_{sorbent}\Delta q < \Delta H_{ads} >}{M_w} \end{aligned}} \tag{11}$$

When we ignore the heat capacity of the condenser, the simplified equation will turn out to be,[2,4]

$$COP_R = \frac{\frac{\Delta H_{vap}(T_{ev})\Delta q}{M_w}}{C_p^{sorbent}(T_{des}-T_1) - \frac{\Delta q < \Delta H_{ads} >}{M_w}} \tag{12}$$

Here the $C_p^{sorbent}$ is assumed to be constant at 1 $kJ/kg.K$. ΔH_{vap} is taken from NIST.[6]

Table. S1: Operating condition for the adsorption refrigeration cycle used in this work

Propane (R-290)	T(K)	P(bar)
Adsorption	313.15	4.7446
Desorption	358.15	10.790

Table. S2: Operating condition for the evaporator and heat exchanger used in this work

Operation	**T(K)**
Evaporator	273.15
Condenser/Heat Exchanger	303.15

S2 COP of the top 20 MOFs

S2.1 Best MOFs

A list of best MOFs with their calculated properties is given in table S3.

Table. S3: COP_R of the best MOFs.

Rank	MOF	$q_{max}(g/g)$	$< H_{ads} > (kJ/mol)$	$\Delta q(g/g)$	Metal atom	COP_R
1	XUKYEI	0.92 ± 0.017	-19.97 ± 1.1	0.252	Cu	0.596
2	QIYDAF01	0.827 ± 0.001	-19.16 ± 1.55	0.166	Cu	0.533
3	XAHPIH	0.818 ± 0.011	-20.753 ± 1.4	0.184	Cu	0.526
4	VETMIS	0.929 ± 0.003	-20.953 ± 0.929	0.181	Cu	0.520
5	CUSXIY	0.7 ± 0.016	-17.19 ± 0.67	0.128	Zn	0.506
6	REZXUQ	0.729 ± 0.009	-20.01 ± 0.523	0.154	Cr	0.503
7	ZELROZ	0.623 ± 0.018	-18.18 ± 0.707	0.125	Zn	0.487
8	LEJCEK	0.765 ± 0.008	-19.95 ± 0.953	0.138	Zn	0.483
9	CUSXOE	0.80 ± 0.001	-16.83 ± 0.67	0.114	Zn	0.483
10	ALEJAE	0.805 ± 0.036	-17.42 ± 0.564	0.116	In	0.480
11	BAZFUF	0.94 ± 0.006	-23.34 ± 0.765	0.177	Cu	0.479
12	ACOCUS	0.899 ± 0.001	-21.12 ± 0.66	0.148	Zn	0.479
13	ADATAC	0.837 ± 0.009	-20.43 ± 0.3	0.139	Zn	0.478
14	BAZFUF01	0.937 ± 0.006	-23.67 ± 0.765	0.177	Cu	0.475
15	ALULEZ	0.590 ± 0.010	-19.9 ± 1.03	0.131	Ce	0.473
16	c6ce00407	0.743 ± 0.005	-19.7 ± 0.49	0.128	Cu	0.471
17	ACOCOM	0.869 ± 0.001	-20.64 ± 0.53	0.136	Cu	0.471
18	BAZGEQ	0.767 ± 0.004	-20.11 ± 1.73	0.131	Cu	0.470
19	XAHPED	0.773 ± 0.010	-22.15 ± 0.835	0.148	Cu	0.467
20	AVAKEP	0.789 ± 0.024	-16.85 ± 0.99	0.106	Cu	0.466

S3 Cooling Capacity(CC)

Top 20 MOFs ranked according to their cooling capacities.

Table. S4: Best MOFs ranked according to cooling capacity

Rank	MOF	Δq (g/g)	COP_R	CC (kJ/kg)
1	XUKYEI	0.252	0.595	94.98
2	XAHPIH	0.184	0.525	69.24
3	VETMIS	0.181	0.520	68.38
4	BAZFUF01	0.177	0.475	66.78
5	BAZFUF	0.177	0.479	66.69
6	QIYDAF01	0.166	0.533	62.64
7	VAGMEX	0.162	0.457	60.919
8	EDUVOO	0.1606	0.459	60.37
9	XAFFER	0.159	0.446	59.94
10	NATKIF	0.158	0.451	59.67
11	XAFFOB	0.157	0.434	59.3
12	XAFFIV	0.156	0.440	58.89
13	REZXUQ	0.153	0.503	57.88
14	AWUPAL	0.150	0.435	56.44
15	XAHPED	0.148	0.467	55.94
16	VAGMAT	0.147	0.422	55.58
17	ACOCUS	0.147	0.479	55.47
18	KUVMIZ	0.147	0.453	55.42
19	XAFFAN	0.145	0.421	54.65
20	AWUPOZ	0.144	0.431	54.48

S4 Pearson Correlation Matrix

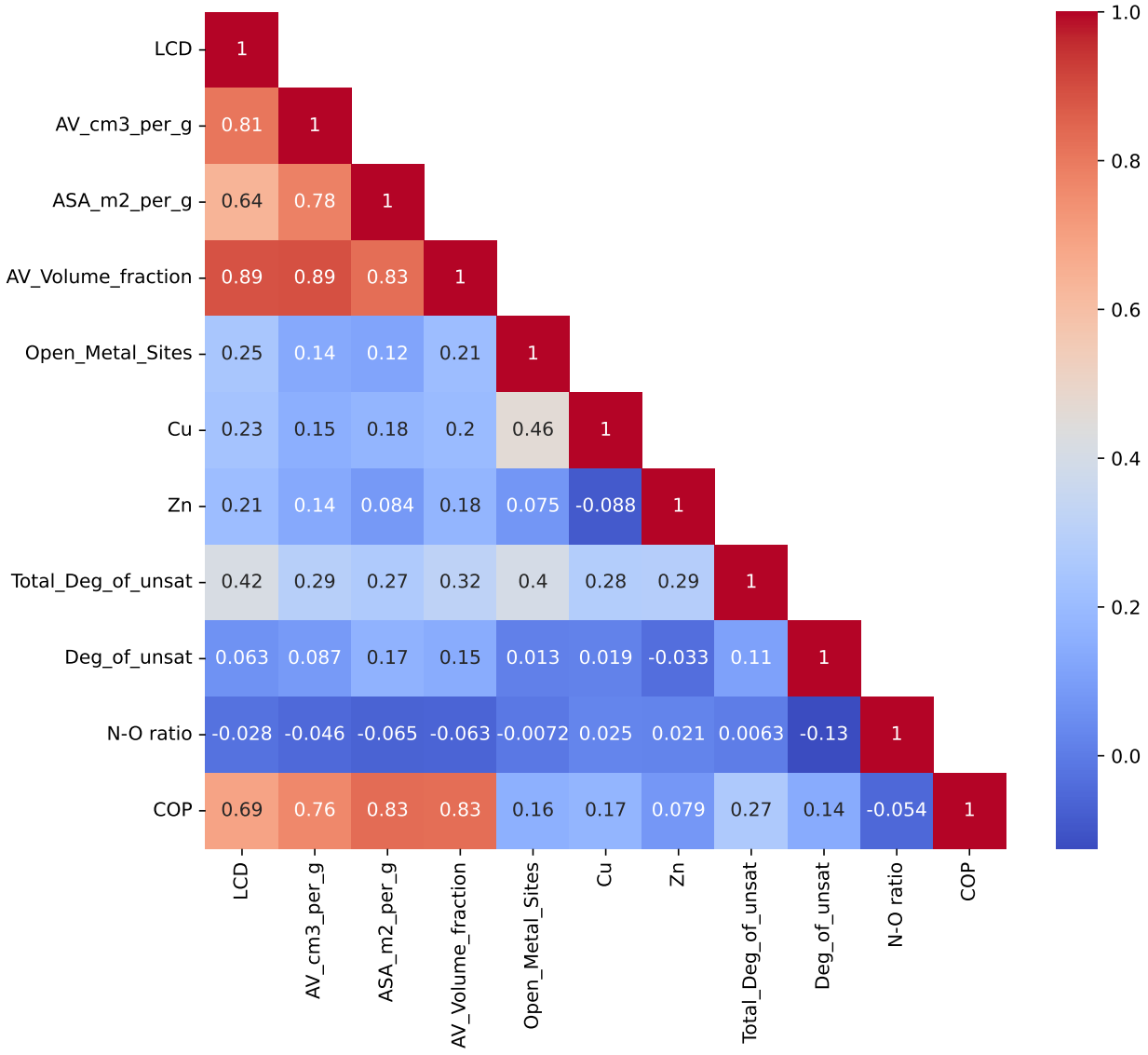

Fig. S3: Pearson Correlation Matrix for COP and properties of a MOF.

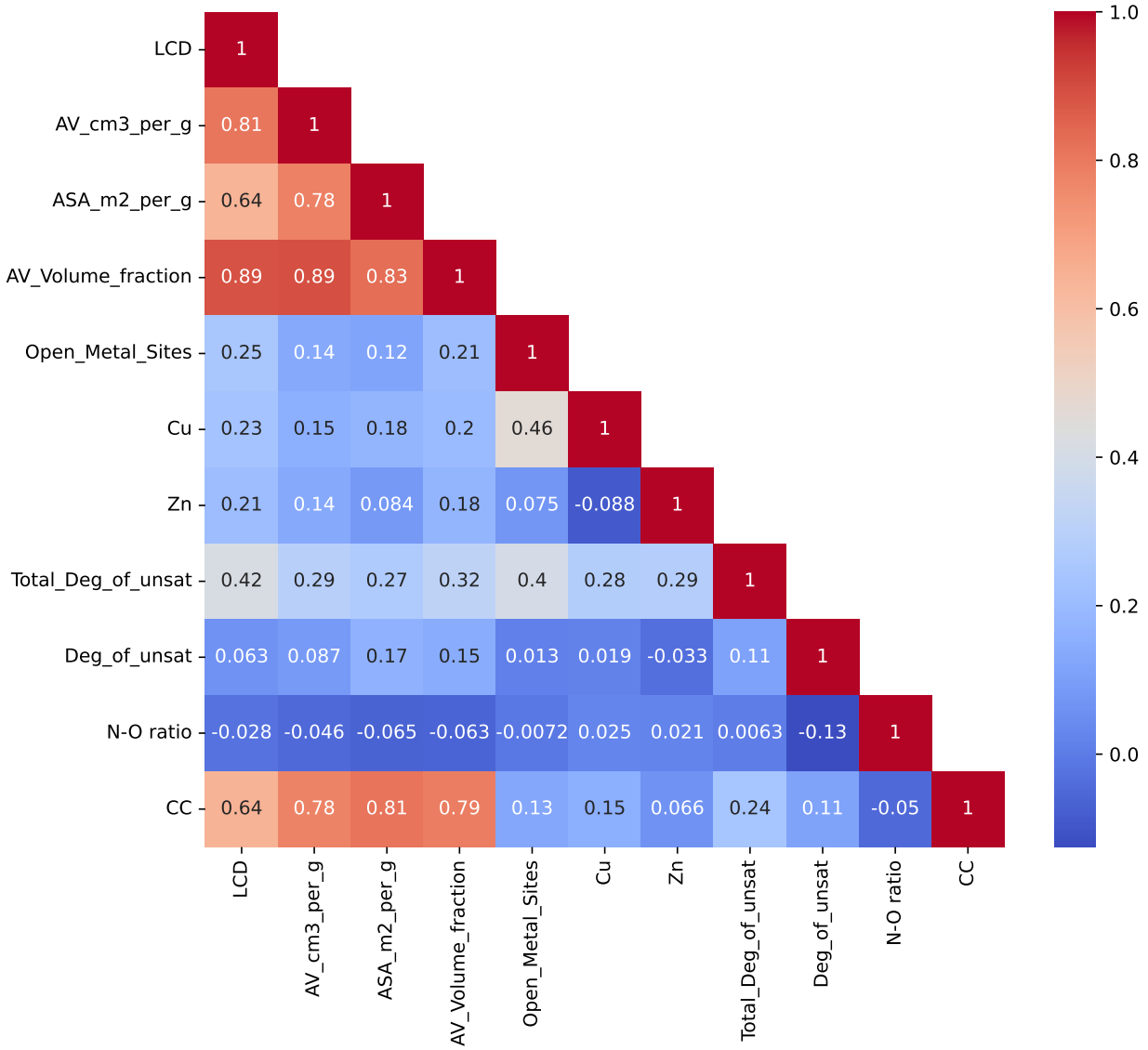

Fig. S4: Pearson Correlation Matrix for CC and properties of a MOF.

S5 Heat Capacity Calculation for MOFs

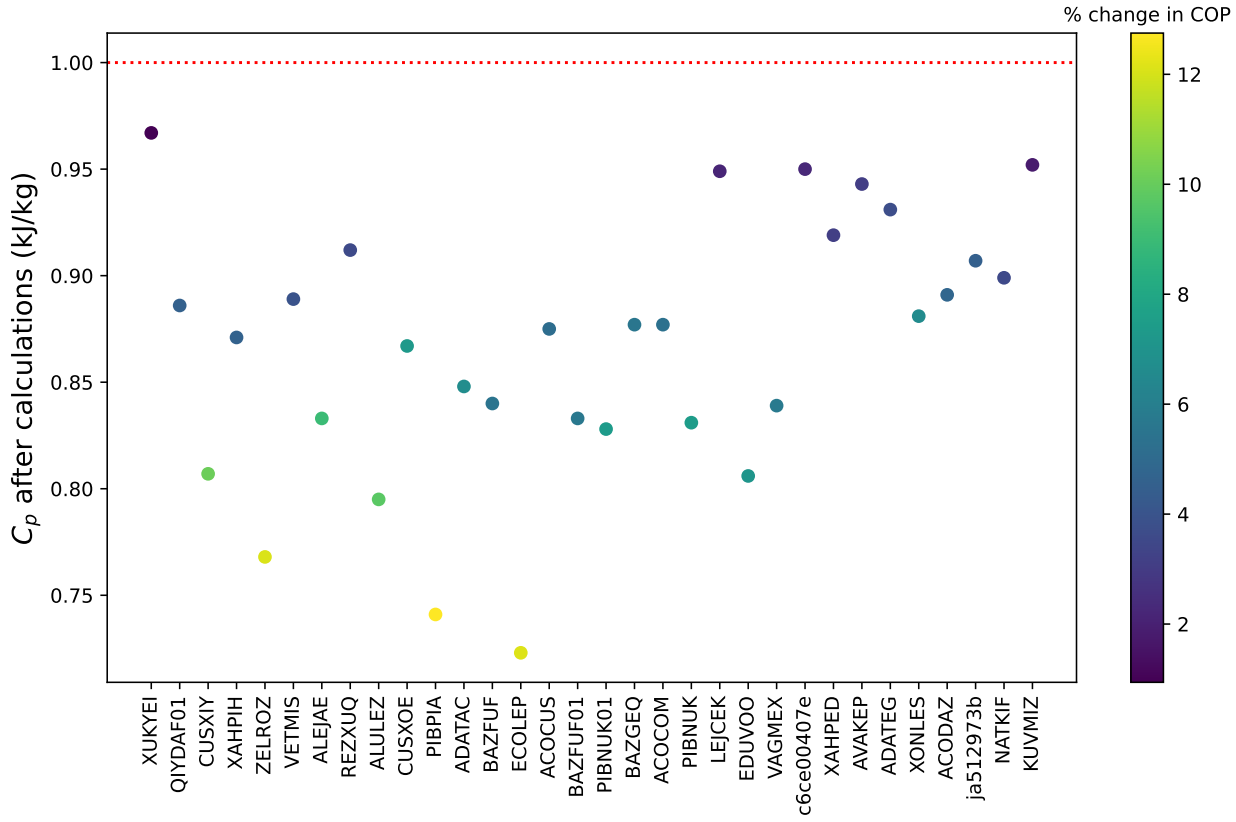

Fig. S5: C_p of MOFs as predicted by machine learning model,[1] colored by percentage change in COP.

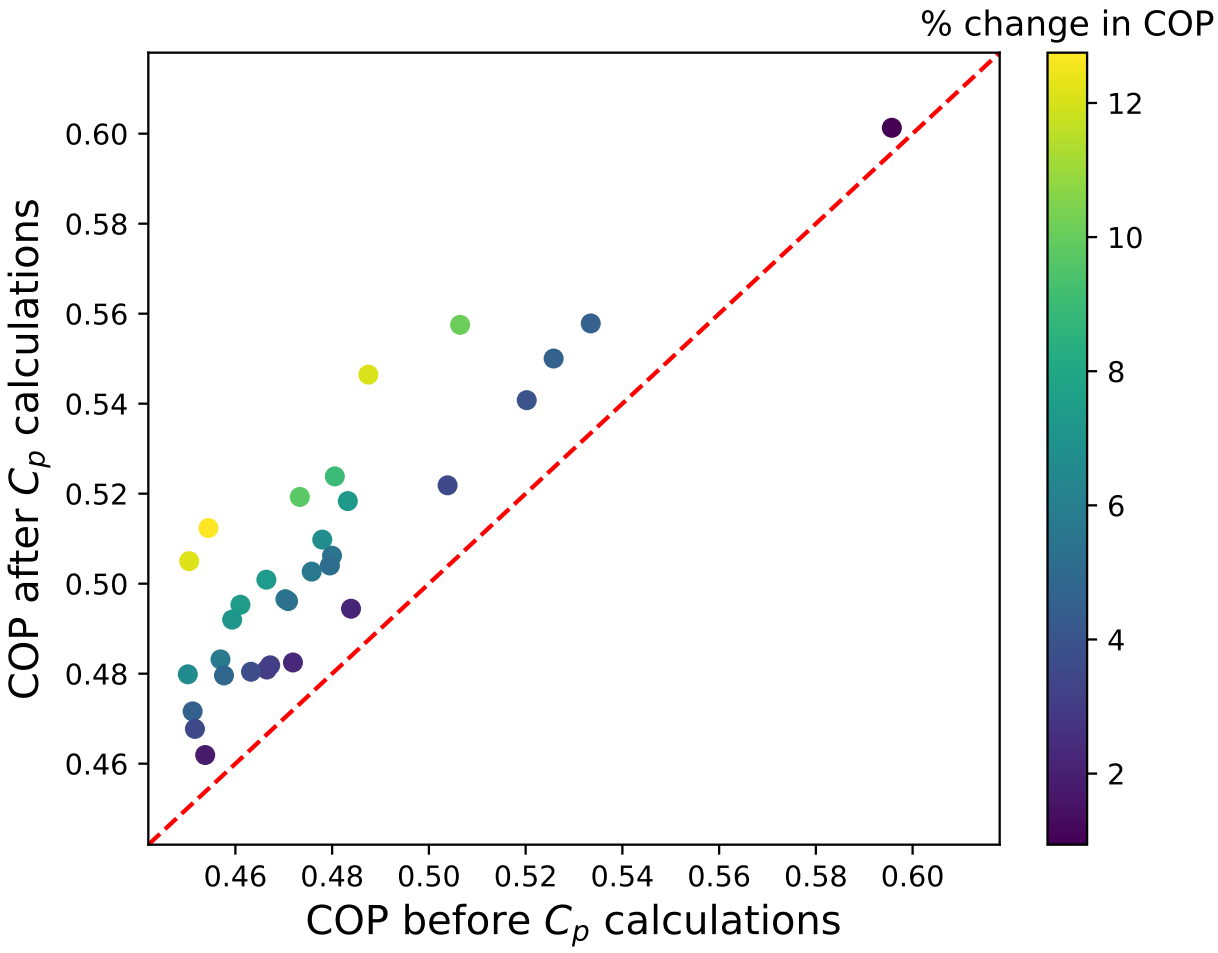

Fig. S6: COP before and after C_p calculations, colored by percentage change in COP.

S6 Optimized Results

The COP and CC after optimization of the cycle are given in the table below.

Table. S5: Comparison of COP before and after optimization, ranked by their optimized COP.

MOF	C_p (kJ/kg K)	COP (before)	COP (after)	% change
CUSXIY	0.81	0.51	0.72	43.08
ALEJAE	0.83	0.48	0.69	44.15
c6ce00407e	0.95	0.47	0.68	43.9
ADATEG	0.93	0.46	0.68	46.38
XUKYEI	0.97	0.6	0.68	13.73
AVAKEP	0.94	0.47	0.68	45.19
QIYDAF01	0.89	0.53	0.66	24.35
ZELROZ	0.77	0.49	0.65	33.05
XONLES	0.88	0.45	0.62	38.55
VETMIS	0.89	0.52	0.62	18.81
REZXUQ	0.91	0.5	0.62	22.33
ALULEZ	0.8	0.47	0.61	29.91
ADATAC	0.85	0.48	0.61	26.92
PIBPIA	0.74	0.45	0.6	31.27
BAZGEQ	0.88	0.47	0.59	26.46
LEJCEK	0.95	0.48	0.59	22.27
EDUVOO	0.81	0.46	0.59	27.62
PIBNUK	0.83	0.46	0.58	26.09
BAZFUF	0.84	0.48	0.58	20.45
ACOCUS	0.88	0.48	0.58	20.03
ECOLEP	0.72	0.45	0.57	27.58

Table. S6: Comparion of CC before and after optimization, ranked by their optimized cooling capacity.

MOF	CC (kJ/kg) (before)	CC (kJ/kg) (after)	% change
XUKYEI	94.98	190.2	100.24
VETMIS	68.38	149.97	119.31
BAZFUF	66.7	147.74	121
QIYDAF01	62.64	146.63	134.07
BAZFUF01	66.79	146.03	118.66
CUSXIY	48.02	134.09	179.23
ECOLEP	51.97	133.53	156.93
VAGMEX	60.92	132.65	117.74
c6ce00407e	48.4	132.04	172.81
ALEJAE	43.71	131.95	201.89
REZXUQ	57.88	131.08	126.46
AVAKEP	39.93	129.34	223.9
ADATEG	40.17	128.92	220.9
NATKIF	59.68	128.63	115.54
ADATAC	52.34	124.28	137.43
CUSXOE	42.69	121.76	185.2
XAHPED	55.95	121.16	116.56
ACOCUS	55.48	120.45	117.11
LEJCEK	52.16	119.85	129.79
KUVMIZ	55.42	117.89	112.71
BAZGEQ	49.3	117.64	138.61

S7 Comparison of cooling capacities

Here, we have compared the cooling capacity obtained in our work with the literature values.

Table. S7: Comparison of Cooling Capacity obtained in this work with the literature values

Pair	$T_{ev}(K)$	$\Delta q(g/g)$	CC (kJ/kg)	COP	References
Refrigerant: Alcohols/water/ammonia					
LiBr-Silica/ethanol	278		200	0.55	[7]
AC/ethanol	278		205	0.54	[7]
SUKYIH/Ethanol	283	0.9	826.35	0.96	[4]
ANUGIA/Ethanol	283	0.82	752.90	0.91	[4]
AC/methanol	278		200	0.59	[7]
Zeolite/methanol	278		180	0.55	[7]
AC-35/methanol	270		239.15		[8]
G-32-H/methanol	270		236.83		[8]
Cr-MIL-101/Water	283	0.143	322.94		[9]
AC/Ammonia	273		108.65		[10]
Refrigerant: Alchols/ water/ ammonia					
XUKYEI/Propane	273	0.51	190.2	0.68	This work
CUSXIY/Propane	273	0.36	134.09	0.72	This work
NU-1000/Propane	278	0.37	141.805		[11]
NU-1003/Propane	278	0.4	153.30		[11]
NU1000/Isobutane	278	0.4	181.42		[11]
NU-1003/Isobutane	278	0.69	312.96		[11]
AC/Isobutane	278		15		[12]
MIL101/Isobutane	278		45		[12]

As shown in the table, only the cooling capacities of the MOF-ethanol pair from Li et al.[4] have exceeded 500 kJ/kg. Generally, working pairs with ethanol, methanol, or water tend to exhibit higher cooling capacities due to their enthalpies of vaporization being nearly three times that of propane or isobutane.

As previously mentioned, the use of alcohols as refrigerants requires meticulous maintenance of vacuum conditions due to their hypobaric vapor pressure,[4,12,13] complicating the practical application of adsorption refrigeration cycles. In contrast, alkane-based refrigerants, with their hyperbaric vapor pressures, facilitate easier implementation in practical applications.

References

(1) Moosavi, S. M.; Novotny, B. Á.; Ongari, D.; Moubarak, E.; Asgari, M.; Kadioglu, Ö.; Charalambous, C.; Ortega-Guerrero, A.; Farmahini, A. H.; Sarkisov, L.; Garcia, S.; Noé, F.; Smit, B. A data-science approach to predict the heat capacity of nanoporous materials. *Nature Materials* **2022**, *21*, 1419–1425, DOI: 10.1038/s41563-022-01374-3.

(2) Nguyen, B. T.; Nguyen, H. L.; Nguyen, T. C.; Cordova, K. E.; Furukawa, H. High Methanol Uptake Capacity in Two New Series of Metal–Organic Frameworks: Promising Materials for Adsorption-Driven Heat Pump Applications. *Chemistry of Materials* **2016**, *28*, 6243–6249, DOI: 10.1021/acs.chemmater.6b02431.

(3) de Lange, M. F.; Verouden, K. J. F. M.; Vlugt, T. J. H.; Gascon, J.; Kapteijn, F. Adsorption-Driven Heat Pumps: The Potential of Metal–Organic Frameworks. *Chemical Reviews* **2015**, *115*, 12205–12250, DOI: 10.1021/acs.chemrev.5b00059, PMID: 26492978.

(4) Li, W.; Xia, X.; Cao, M.; Li, S. Structure–property relationship of metal–organic frameworks for alcohol-based adsorption-driven heat pumps via high-throughput computational screening. *J. Mater. Chem. A* **2019**, *7*, 7470–7479, DOI: 10.1039/C8TA07909A.

(5) Farmahini, A. H.; Limbada, K.; Sarkisov, L. Comment on the applicability of the Gurvich rule for estimation of pore volume in microporous zeolites. *Adsorption* **2022**, *28*, DOI: 10.1007/s10450-022-00364-w.

(6) Linstrom, P. J.; Mallard, W. G. The NIST Chemistry WebBook: A Chemical Data Resource on the Internet. *Journal of Chemical & Engineering Data* **2001**, *46*, 1059–1063, DOI: 10.1021/je000236i.

(7) Freni, A.; Maggio, G.; Sapienza, A.; Frazzica, A.; Restuccia, G.; Vasta, S. Comparative analysis of promising adsorbent/adsorbate pairs for adsorptive heat pumping, air

conditioning and refrigeration. *Applied Thermal Engineering* **2016**, *104*, 85–95, DOI: https://doi.org/10.1016/j.applthermaleng.2016.05.036.

(8) Hadj Ammar, M.; Benhaoua, B.; Bouras, F. Thermodynamic analysis and performance of an adsorption refrigeration system driven by solar collector. *Applied Thermal Engineering* **2017**, *112*, 1289–1296, DOI: https://doi.org/10.1016/j.applthermaleng.2016.09.119.

(9) Canivet, J.; Fateeva, A.; Guo, Y.; Coasne, B.; Farrusseng, D. Water adsorption in MOFs: fundamentals and applications. *Chem. Soc. Rev.* **2014**, *43*, 5594–5617, DOI: 10.1039/C4CS00078A.

(10) Critoph, R. An ammonia carbon solar refrigerator for vaccine cooling. *Renewable Energy* **1994**, *5*, 502–508, DOI: https://doi.org/10.1016/0960-1481(94)90424-3, Climate change Energy and the environment.

(11) Chen, H.; Chen, Z.; Farha, O. K.; Snurr, R. Q. High Propane and Isobutane Adsorption Cooling Capacities in Zirconium-Based Metal–Organic Frameworks Predicted by Molecular Simulations. *ACS Sustainable Chemistry & Engineering* **2019**, *7*, 18242–18246, DOI: 10.1021/acssuschemeng.9b05368.

(12) Ma, L.; Yang, H.; Wu, Q.; Yin, Y.; Liu, Z.; Cui, Q.; Wang, H. Study on adsorption refrigeration performance of MIL-101-isobutane working pair. *Energy* **2015**, *93*, 786–794, DOI: https://doi.org/10.1016/j.energy.2015.09.097.

(13) García, E. J.; Bahamon, D.; Vega, L. F. Systematic Search of Suitable Metal–Organic Frameworks for Thermal Energy-Storage Applications with Low Global Warming Potential Refrigerants. *ACS Sustainable Chemistry & Engineering* **2021**, *9*, 3157–3171, DOI: 10.1021/acssuschemeng.0c07797.